

# Application of nanofibers to improve the filtration efficiency of the most penetrating aerosol particles in fibrous filters

Albert Podgórski\*, Anna Bałazy, Leon Gradoń

*Faculty of Chemical and Process Engineering, Warsaw University of Technology, Ul. Waryńskiego 1, 00-645 Warsaw, Poland*

Received 24 November 2005; received in revised form 7 July 2006; accepted 13 July 2006

Available online 18 July 2006

## Abstract

Conventional, mechanical fibrous filters made of microfibers exhibit a local minimum of fractional collection efficiency in the aerosol particle size-range between 100 and 500 nm, which is called the most penetrating particle size (MPPS). Simple theoretical calculations predict that this efficiency may be significantly increased using nanofibrous media. The main objective of this paper is an experimental verification of these expectations and simultaneously checking whether this anticipated gain in the filtration efficiency is not overpaid with an excessive pressure drop. For this purpose we developed a modified melt-blown technology, which allowed us to produce filters composed of micrometer as well as nanometer sized fibers. One conventional microfibrous filter and five nanofibrous filters were examined. The complete structural characteristics, pressure drop and efficiency of removal of aerosol particles with diameters 10–500 nm were determined for all media. The results of the experiments confirmed that using nanofibrous filters a significant growth of filtration efficiency for the MPPS range can be achieved and the pressure drop rises moderately. Simultaneously, we noticed a shift of the MPPS towards smaller particles. Consequently, the quality factor for bilayer systems composed of a microfibrous support and a nanofibrous facial layer was considerably higher than this one for a conventional microfibrous filter alone. Additionally, it was found that utilization of many-layer nanofibrous filters combined with a single microfibrous backing layer is even more profitable from the quality factor standpoint. Comparing experimental results with theoretical calculations based on the single-fiber theory we concluded that for microfibrous filters a fairly good agreement can be obtained if the resistance-equivalent fiber diameter is used in calculations instead of the mean count diameter determined from the SEM images analysis; in the latter case, filtration efficiency computed theoretically is slightly overestimated. This is even more evident for nanofibrous media, suggesting that in such case a structural filter inhomogeneity has a strong influence on the filter efficiency and its resistance and one should strive for minimization of this effect manufacturing nanofibrous filters as homogeneous as possible. We can finally conclude that fibrous filters containing nanofibers, which are produced using the melt-blown technique, are very promising and economic tools to enhance filtration of the most penetrating aerosol particles. © 2006 Elsevier Ltd. All rights reserved.

**Keywords:** Aerosol; Efficiency; Filtration; Nanofibers; Particle; Separations

## 1. Introduction

Fibrous filters are typically manufactured with the fibers of diameters about a few dozen micrometers, and the filter porosity is usually 80–90%. Such structure allows removing sub-micrometer and micrometer particles with a high efficiency, maintaining a relatively low resistance to the air flow. However, there is the size-range of the particles that are not filtered out as efficiently as other particles. The fibrous filter efficiency

achieves a minimum at so-called the most penetrating particle size (MPPS), which is usually between 0.1 and 0.5  $\mu\text{m}$  for mechanical filters. Theoretical predictions and preliminary investigations indicate that significant increase of the filter efficiency for the MPPS, accompanied by only a slight rise of the pressure drop, may be achieved by using the nanometer fibers to produce the fibrous filters (Hinds, 1999; Grafe et al., 2001). Nomenclature concerning objects with the size of nanometers is still not clearly defined and may be somewhat confusing. In the case of particles, these that have diameter smaller than 0.1  $\mu\text{m}$  (100 nm) are considered as nanoparticles (Aitken et al., 2004). However, some authors define the term “nanoparticles”

\* Corresponding author. Tel.: +48 22 660 63 51; fax: +48 22 825 14 40.

E-mail address: [podgorski@ichip.pw.edu.pl](mailto:podgorski@ichip.pw.edu.pl) (A. Podgórski).

in a different manner, limiting the upper size of nanoparticles to 50 nm (Hinds, 1999) or even 40 nm (ISO, 2004). Contrary to these definitions, as “nanofibers” generally fibers with diameter less than 1  $\mu\text{m}$  are considered (Grafe et al., 2001; Graham et al., 2002). In this paper, the filters that have at least some fraction of fibers with diameter below 1  $\mu\text{m}$  will be called “nanofibrous medium”.

Nanofibers are characterized by a very large surface area to volume ratio, which significantly increases the probability of the aerosol particles deposition on the fiber surface and thereby improves the filter efficiency (Huang et al., 2003; Park and Park, 2005). Filters composed of nanofibers provide high filtration efficiency of the particles with the MPPS at relatively low pressure drops.

In addition to a large surface area to volume ratio, the nanofibrous media have low basis weight, high permeability, and tight pore size that make them appropriate for a wide range of filtration applications. There are three major processes for producing nanofibers for filtration media: electrostatic spinning, melt-blown technique, and multicomponent fiber spinning or the ‘islands-in-the sea’ method (Ward, 2005). Currently, the nanofibers are mostly produced using electrospinning technology. The fibers made by electrospinning have in general diameter in the range 0.04–2  $\mu\text{m}$  (Grafe and Graham, 2002; Kosmider and Scott, 2002; Park and Park, 2005); however, it may be found in the literature that using electrospinning method fibers less than 3 nm can be produced (Huang et al., 2003). The diameter of the fibers depends, among other things, on the polymer solution concentration. The thinner fibers may be achieved using less concentrate solution. However, decrease of the solution concentration increases the amount of hazardous vapors emitted from electrospinning solution while forming the fibers that need to be recovered or disposed of, and this involves additional equipment and cost (Jaroszczyk et al., 2005). The drawbacks of this process, besides the hazardous vapors emission, are that the production rate is very slow, thus the product is expensive (Jaroszczyk et al., 2005; Kalayci et al., 2005), some polymers are difficult to dissolve (Ward, 2005), the fiber diameters obtained are seldom uniform (Demir et al., 2002), and nanofibers may have defects like beads and pores (Huang et al., 2003).

Electrospun fibers have diameters smaller than that of melt-blown fibers; however, currently there are investigations aimed at improving of the latter technique to produce nanofibers. The melt-blown technique may allow making large quantities of such fibers at low cost, which will considerably increase their commercial applications.

In our study the filters containing fibers of diameter as small as 0.2  $\mu\text{m}$  were manufactured by the melt-blown method. Since nanofibrous media have weak mechanical properties, they were used with additional microfibrinous support. We investigated the performance of self-manufactured filters composed of the fibers, which some fraction had diameter below 1  $\mu\text{m}$  (nanofibrous filters). The filtration efficiencies of the sets of

microfibrinous filter covered by layer of nanofibrous media were tested against liquid particles with diameter from 10 to 500 nm.

## 2. Materials and methods

This section begins with a simple theoretical analysis of the performance of microfibrinous and nanofibrous filter media, which suggests that a significant increase in a filter quality factor for the range of the most penetrating particles can be achieved if nanofibrous filters are used. Then, the method of production of such media and the experimental protocol used to study their performance are briefly described.

### 2.1. Preliminary theoretical analysis

Properly designed fibrous filter should first of all assure a high efficiency of aerosol particles removal,  $\eta$ , maintaining simultaneously the pressure drop,  $\Delta p$ , at a level as low as possible. Both these crucial parameters depend, although in a different way, on such filter’s properties, like its thickness,  $L$ , porosity,  $\varepsilon$ , and the fiber diameter,  $d_F$ . The quality factor, QF, which is defined as

$$\text{QF} = \frac{-\ln(1 - \eta)}{\Delta p}, \quad (1)$$

is the commonly used quantitative criterion to compare various fibrous filters, see, for example, Dorman (1966) or Brown (1993). A more realistic rating should take into consideration variation in the pressure drop and in the filtration efficiency during continuous loading of a filter with deposits. The appropriate criterion based on economic rules that accounts for these phenomena, the filter utility factor  $FUF$ , was proposed by Podgórski (2002). The filter efficiency,  $\eta$ , is calculated based on the upstream,  $c_{\text{up}}$ , and downstream,  $c_{\text{down}}$ , aerosol concentration as follows:

$$\eta = \frac{c_{\text{up}} - c_{\text{down}}}{c_{\text{up}}}. \quad (2)$$

The aim of this section is to estimate theoretically whether the use of ultrafine fibers would be profitable for the process of filtration of submicrometer and nanometer aerosol particles. Especially, we would like to check if it is possible to gain a substantial improvement in the filtration efficiency for the most penetrating particles and simultaneously to assess whether the use of ultrafine fibers is favorable for this size-range from the QF criterion standpoint. For this purpose we made some simple estimates using the commonly known equations formulated in the classical theory of depth filtration. Since we consider only particles smaller than 500 nm in diameter, we limited our analysis to two predominating then mechanisms of deposition, i.e., the Brownian diffusion (labeled “D”) and the direct interception (“IR”). The single-fiber deposition efficiencies for these two mechanisms,  $E_D$  and  $E_{\text{IR}}$ , respectively, were calculated from the following formulae, see Gougeon et al. (1996):

$$E_D = \frac{1.6((1 - \alpha)/Ku)^{1/3}Pe^{-2/3}[1 + 0.388Kn_F((1 - \alpha)Pe/Ku)^{1/3}]}{1 + 1.6((1 - \alpha)/Ku)^{1/3}Pe^{-2/3}[1 + 0.388Kn_F((1 - \alpha)Pe/Ku)^{1/3}]}, \quad (3)$$

Table 1  
Structural characteristics of the analyzed filters

Filter no.	$L$ (mm)	$d_F$ ( $\mu\text{m}$ )	$\alpha$ [dimensionless]	$\rho_{SF}$ ( $\text{g}/\text{m}^2$ )	$a_F$ ( $\text{m}^2/\text{m}^3$ )
1	3	10	0.1	273	$4 \times 10^4$
2	1	2	0.05	45.5	$10^5$
3	1	0.7	0.02	18.2	$1.14 \times 10^5$
4	0.2	0.1	0.005	0.91	$2 \times 10^5$

$$E_{\text{IR}} = 0.6 \left( \frac{1 - \alpha}{Ku} \right) \left( \frac{\text{IR}^2}{1 + \text{IR}} \right) \left( 1 + \frac{1.996Kn_F}{\text{IR}} \right). \quad (4)$$

In the above equations  $\alpha$  denotes the filter packing density,  $\alpha = 1 - \varepsilon$ , and the dimensionless numbers are defined as follows:

- Peclet number  $Pe = \frac{Ud_F}{D}$ ;
- Knudsen number for fiber  $Kn_F = \frac{2\lambda_g}{d_F}$ ;
- Kuwabara number  $Ku = \frac{-\ln \alpha}{2} - \frac{3}{4} + \alpha - \frac{\alpha^2}{4}$ ;
- Interception parameter  $\text{IR} = \frac{d_p}{d_F}$ .

$U$  denotes here face gas velocity,  $D$  the coefficient of Brownian diffusion for a particle,  $\lambda_g$  the gas mean free path, and  $d_p$  the aerosol particle diameter.

Assuming that Brownian diffusion and direct interception are independent mechanisms of deposition, the total single-fiber deposition efficiency,  $E$ , due to the action of both of them was calculated as

$$E = 1 - (1 - E_D)(1 - E_{\text{IR}}). \quad (5)$$

In the next step the single-fiber efficiency  $E$  was recalculated into the filter efficiency,  $\eta$ , according to well-known formula

$$\eta = 1 - \exp \left( \frac{-4\alpha EL}{\pi d_F(1 - \alpha)} \right). \quad (6)$$

To calculate the pressure drop across a filter we used the theoretical equation reported in Brown's (1993) handbook, which is based on the Kuwabara flow model with a gas slip:

$$\frac{\Delta p}{L} = \frac{U\alpha\mu L(1 + 1.996Kn_F)}{d_F^2[Ku + 1.996Kn_F(Ku - \alpha + 0.5(1 + \alpha^2))]} \quad (7)$$

Alternatively,  $\Delta p$  may be estimated from the commonly used empirical correlation developed by Davies (1973):

$$\frac{\Delta p}{L} = \frac{64\mu U}{d_F^2} \alpha^{3/2} (1 + 56\alpha^3). \quad (8)$$

Theoretical calculations were made for four various fibrous filters, which characteristics are collected in Table 1. The filter #1 is the thickest one ( $L = 3$  mm), made of the most coarse fibers ( $d_F = 10$   $\mu\text{m}$ ) and it is the most densely packed ( $\alpha = 0.1$ ). The filters #2 and #3 have the same, smaller than the filter #1, thickness ( $L = 1$  mm). Among them the filter #3 is more porous and contains finer fibers than the filter #2. Finally, the filter #4 is the thinnest one ( $L = 0.2$  mm), extremely porous ( $\alpha = 0.005$ ) and made of the thinnest fibers ( $d_F = 0.1$   $\mu\text{m}$ ). In addition to the filter thickness, fiber diameter and the filter packing density, the

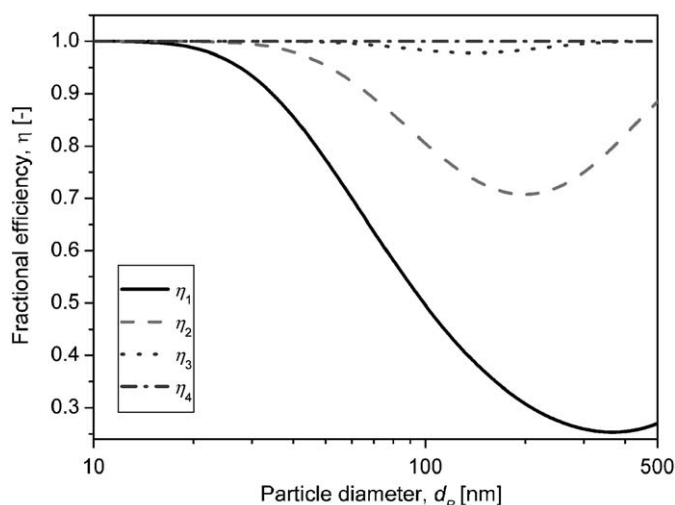


Fig. 1. Calculated fractional efficiency for four considered filters (subscript in the legend denotes filter number) as a function of aerosol particle diameter.

filter surface density (basis weight, i.e., mass of the filter per its surface area),  $\rho_{SF}$ , and the filter specific area (i.e., the total area of fibers per filter volume),  $a_F$ , are also reported in Table 1. These parameters were calculated as follows:  $\rho_{SF} = L\alpha\rho_F$  and  $a_F = 4\alpha/d_F$ , assuming that the density of the fibers' material is the same as for polypropylene,  $\rho_F = 910$   $\text{kg}/\text{m}^3$ . Note that the filters containing finer fibers, although being thinner and more porous, have greater specific area but simultaneously smaller surface density.

All theoretical calculations presented in this section were done for superficial air velocity  $U = 0.1$  m/s. Fig. 1 shows fractional efficiency for four analyzed filters determined in accordance with Eqs. (3)–(7) for the range of aerosol particle diameters 10–500 nm, i.e., the same as that one in the experimental studies discussed henceforth. The MPPS was found to be 366 nm for the filter #1, 199 nm for the filter #2, 140 nm for the filter #3, and 54 nm for the filter #4. This shift of the MPPS towards smaller particle sizes observed for filters composed of thinner fibers may be easily explained by the fact that in the case of finer fibers a net with much smaller meshes is formed, thus the efficiency of particle removal due to direct interception is significantly increased for submicrometer particles. And secondly, one can observe in Fig. 1 a very promising growth of the fractional efficiency in the entire range of particle sizes, but especially meaningful in the vicinity of the MPPS. The maximal value of the aerosol penetration,  $P_{\text{max}}$ , for the filter #1 made of 10  $\mu\text{m}$  fibers is as high as 0.747 and it gradually decreases for filters composed of finer fibers, reaching only  $3.28 \times 10^{-4}$  for the filter #4 consisting of 100 nm fibers, cf. Table 2. Therefore, we can conclude that utilization of nanofibers to manufacture air filters seems to be an excellent solution from the standpoint of the filter efficiency improvement, especially if the process target is removal of submicrometer-sized aerosol particles, usually being the hardest to filter out. However, a question arises whether such a solution is profitable since a gain in filtration efficiency in nanofibrous media will be paid with an increase

Table 2  
Calculated filters' performance at air face velocity  $U = 0.1$  m/s

Filter no.	$MPPS$ (nm)	$P_{max}$ [dimensionless]	$QF_{min}$ (Pa <sup>-1</sup> )	$\Delta p$ (Pa)
1	366	0.747	$1.69 \times 10^{-3}$	173
2	199	0.293	$2.85 \times 10^{-3}$	431
3	140	0.0222	$4.32 \times 10^{-3}$	882
4	54	$3.28 \times 10^{-4}$	$6.20 \times 10^{-3}$	1295

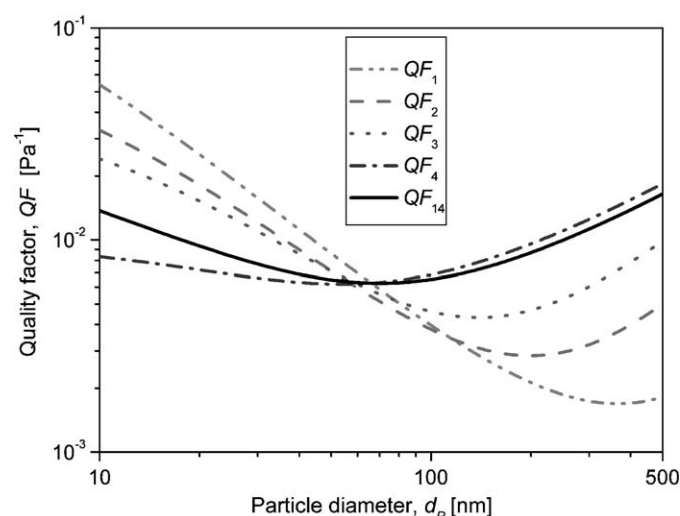


Fig. 2. The filter quality factor computed for four analyzed filters ( $QF_1$ – $QF_4$ ) and for the bilayer system ( $QF_{14}$ ) as a function of aerosol particle diameter.

in the filter resistance. Actually, the pressure drop for the filter #4 calculated from Eq. (8) is seven-and-a-half-fold greater than the pressure drop for the filter #1, see Table 2. Thus, to judge which of the analyzed filters is the best one, we calculated the values of the fractional quality factor according to Eq. (1) and these results are presented in Fig. 2. The final assessment depends on the size distribution of aerosol particles to be filtered. As seen in Fig. 2, the quality factor for the filter #4 is lower than for the other ones for particle diameters below 60–70 nm. This means that use of nanofibrous media is unjustified if only such small nanoparticles are contained in the challenging aerosol stream. The explanation of this finding is rather obvious. Very small nanoparticles are effectively filtered even in conventional, microfibrillar filters due to very efficient mechanism of Brownian diffusion, therefore the use of a nanofibrous layer with an elevated pressure drop makes no sense in this case. However, this is rather unlikely scenario—in reality, a polydispersed aerosol usually undergoes separation, ergo, one should pay a special attention to effective removal of the most penetrating particles. From this point of view, the use of nanofibrous media seems to be irreplaceable. We can observe in Fig. 2 that the quality factor for the filter #4 is nearly an order of magnitude higher than  $QF$  for the conventional filter #1 for the particle size-range 300–400 nm, commonly considered to be the  $MPPS$ . Note also that the calculated minimum value of the quality factor,  $QF_{min}$ , decreases with the increase of the

fiber diameter, being 3.7 times higher for the filter #4 than for the filter #1, see Table 2. A weak point of thin, porous, nanofibrous media may be their mechanical strength and durability. Thus, we recommend combining a layer containing nanofibers with a thicker layer composed of micrometer-sized fibers, serving as a support. Results of calculations of the quality factor for such a bilayer system with the filter #1 placed at the rear of the composite and the filter #4 mounted in front are also shown in Fig. 2. It can be observed that the quality factor for the set of filters #1 and #4 is almost as high as for the filter #4 alone for particle diameters greater than 70 nm, while for smaller particles it is substantially higher than for the single layer of the filter #4. Therefore, the use of nanofibrous filters in combination with conventional microfibrillar support is especially profitable in the case of filtration of a polydispersed aerosol containing nanosized and submicrometer-sized particles.

Calculations presented in this section are based on the simplest single-fiber theory that assumes the same size of all fibers and perfectly homogeneous filter structure. Real filters are always more or less inhomogeneous and are composed of polydisperse fibers. This results in a lower pressure drop and a lower efficiency of a real filter than predicted by the theory.

## 2.2. Method of production of nanofibrous filter media

The scheme of the stand for obtaining fibers by blowing a melted polymer is shown in Fig. 3(a), and in Fig. 3(b) some details of the die construction are shown (a polymer stream is denoted there by 1 and the air stream by 2).

Granulated polymer placed in a container 1 is taken by the screw of the extruder 2 and pressed into the die 6. During transportation the polymer is heated from outside in three steps by an electronic heater 3. The flow rate of melted and homogenized polymer is determined by the rate of the screw rotation controlled via inverter through an electronic motor with the gear system 4. The power transmission system is protected from the heating zone by the cooling system 5. The melted polymer is extruded through the row of the die nozzles (Fig. 3(b)). Pressure and temperature of the polymer in the die are measured with the sensing elements 9. In the die structure the polymer nozzles are surrounded by the air nozzles. The stream of hot air from compressor 7 flowing along melted polymer filaments extends them to the desired diameter. The solidified fibers are collected on the mandrel of fibers receiver 8. This mandrel rotates and moves to-and-fro to form a proper filter structure, defined by the fiber diameter and the local packing density of fibers.

It would be desirable to model the process of single-fiber formation in the melt-blown technology for better understanding of its principles and for optimization of the operating conditions of the fiber manufacture to get finally expected filter structure.

Let us consider a single hole of the die, Fig. 4, and polymer flowing with volumetric flow rate  $Q$  through it. After leaving the hole a melted fiber of radius  $R$  is formed.

The basic information describing formation of a thin fiber in the melt-blown technology are derived under the following



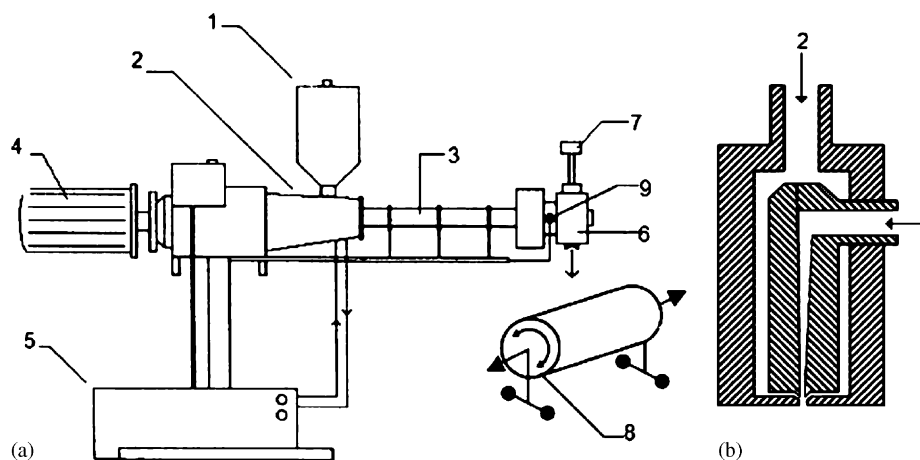


Fig. 3. Production line of nanofibrous material.

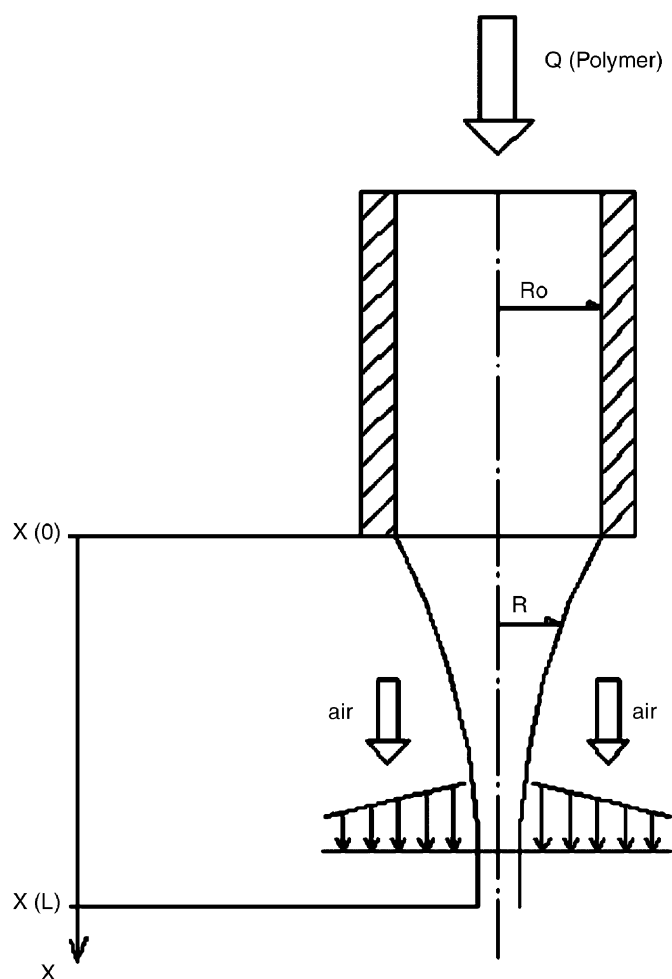


Fig. 4. Schematic of a single-fiber formation.

assumptions: a fiber has a cylindrical shape, a polymer has the same density for melted and solid phases, an axial velocity within a melted fiber is uniform in the fiber cross-section, polymer is a Newtonian liquid with Arrhenius type of dependence

of viscosity on temperature, the heat capacity of the polymer is constant, the temperature distribution is uniform in the fiber cross-section, the heat conduction in the axial direction is negligible.

Taking into account constancy of the polymer volumetric flow rate, balancing the momentum, and using the stress-strain relations and energy balances, we were able to estimate the influence of the process parameters on the properties of the final product (Gradoń et al., 2005). Theoretical analysis of the single-fiber formation gives the quantitative information about the radius  $R$  of the solidified polymer fiber at the distance  $x$  from the nozzle hole of radius  $R_0$  for precisely fixed model parameters, i.e., polymer constitutive properties, flow rates and temperatures of polymer and air, and polymer pressure in the die.

With these information the process parameters for the melt-blown technology were defined. For a fixed set of process parameters the desired filter layers were produced and used in the filtration testing procedure.

### 2.3. Characteristics of the filter media and experimental setup

Six polypropylene fibrous filters were produced using the technology described in the previous section and the complete structural characteristics of these filters were determined. We intended to manufacture one conventional microfibrillar filter (it will be called the backing layer, BL, hereinafter) and five filters consisting predominantly of much finer, preferably nanometer-sized fibers (these five filters will be consecutive labeled as nanofibrous layer #1, NL1,..., nanofibrous layer #5, NL5).

A few rectangular samples of each filter with sizes around  $4 \times 4$  cm were prepared and all their dimensions were measured using a precise vernier caliper. In this way the filter thickness,  $L$ , and the surface area,  $A_F$ , of each sample were determined. In addition, mass of each sample,  $m_F$ , was measured with a precision balance. The surface density (basis weight),  $\rho_{SF}$ , was calculated as:  $\rho_{SF} = m_F / A_F$ , and then the filter porosity,  $\varepsilon$ , was determined according to the formula:

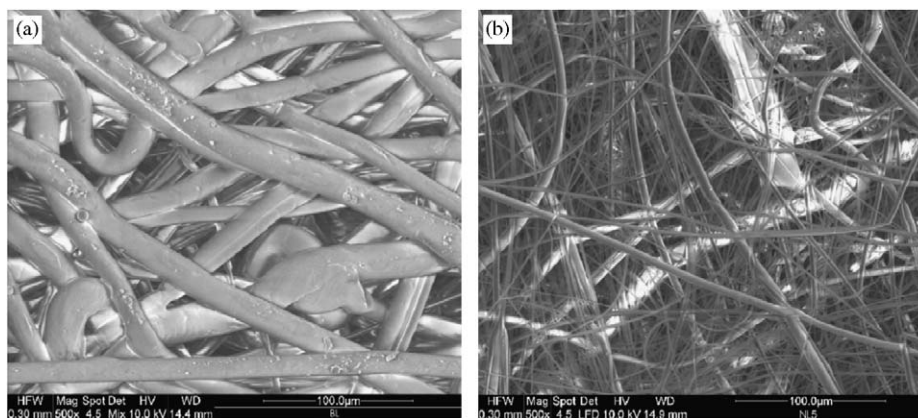


Fig. 5. SEM pictures of the backing layer (a) and the nanofibrous layer #5 (b).

Table 3  
Macroscopic structural characteristics of the manufactured filters

Type of filter	Thickness $L$ (mm)	Porosity $\varepsilon$ [dimensionless]	Basis weight $\rho_{SF}$ (g/m <sup>2</sup> )
Backing layer (BL)	2.1	0.851	284.9
Nanofibrous layer 1 (NL1)	1.4	0.965	44.4
Nanofibrous layer 2 (NL2)	2.5	0.967	75.1
Nanofibrous layer 3 (NL3)	3.1	0.971	79.4
Nanofibrous layer 4 (NL4)	5.5	0.980	100.5
Nanofibrous layer 5 (NL5)	4.3	0.986	53.0

$\varepsilon = 1 - \rho_{SF}/(\rho_F L)$ , wherein  $\rho_F$  is the fibers' material density (910 kg/m<sup>3</sup> for polypropylene was used). Results of such macroscopic analysis are summarized in Table 3. Amongst the nanofibrous filters, the NL1 ( $L = 1.4$  mm) was the thinnest one and the NL4 ( $L = 5.5$  mm) was the thickest one; the backing layer BL had an intermediate thickness ( $L = 2.1$  mm). On the other hand, the BL was the most densely packed filter (its porosity was only 0.851), while all the nanofibrous layers were much more porous ( $\varepsilon$  ranged from 0.965 for the NL1 to 0.986 for the NL5). Consequently, the basis weight of the BL (284.9 g/m<sup>2</sup>) was significantly higher than that for all NLs (which varied between 44.4 g/m<sup>2</sup>, for the thinnest filter NL1, and 100.5 g/m<sup>2</sup> for the NL4, being the thickest one).

To characterize the fiber size distribution, SEM photographs of all filters were taken and then the diameters of all fibers visible on the pictures were measured. Fig. 5 shows two exemplary SEM pictures for the BL and for the NL5. Determined distributions of the fiber diameters are shown for all filters in Fig. 6 and essential parameters of these distributions, like arithmetic mean (count mean) fiber diameter,  $d_{FC}$ , median,  $d_{F,med}$ , standard deviation, SD, and coefficient of variation, CV, of the distributions, and observed range of fibers diameters, are collected in Table 4. The backing layer BL was composed of fibers with diameters in the range 10.2–37.5 µm, while all nanofibrous layers contained fibers with diameters between a few hundreds of nanometers and a few micrometers. The mean diameter of the BL was equal to 18 µm and the median diameter 16 µm. Among the nanofibrous layers the NL1 and the NL2 had rela-

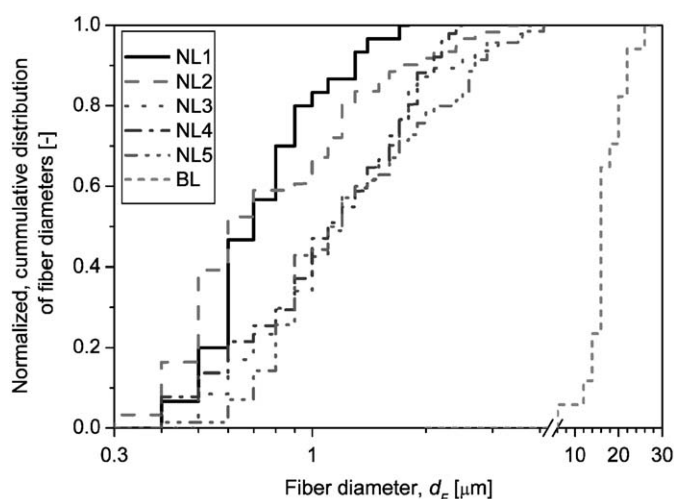


Fig. 6. Fiber size distributions of the manufactured filters.

tively largest fraction of fibers with  $d_{FC} < 1$  µm. The NL1 had the smallest value of the mean fiber diameter (740 nm), but the median fiber diameter was the smallest for the NL2 (600 nm), which also contained the finest fibers amongst of all analyzed filters, with diameters starting from 210 nm. On the other hand, the size distribution of fibers for the NL2 was broader compared to that one for the NL1. Three other nanofibrous layers, NL3, NL4 and NL5, were characterized by almost the same median fiber diameter ( $\sim 1.1$  µm), larger than these for the NL1 and the NL2; the mean fiber diameter ranged between 1.18 µm for NL4 and 1.41 µm for the NL5, which was the highest value for all nanofibrous layers. A degree of the fibers' polydispersity can be characterized by the coefficient of variation, CV, defined as the ratio of the standard deviation of fibers size distribution, SD, to the mean fiber diameter. From this viewpoint, the least polydisperse filters were the BL and the NL1, having values of CV equal to 0.38 and 0.41, respectively. The most polydisperse filter was the NL2 (i.e., the one that had the biggest fraction of the finest fibers), which was characterized by CV = 0.72. Other nanofibrous layers, NL3, NL4 and NL5, were also relatively highly polydisperse with CV ranging between 0.5 and 0.6.



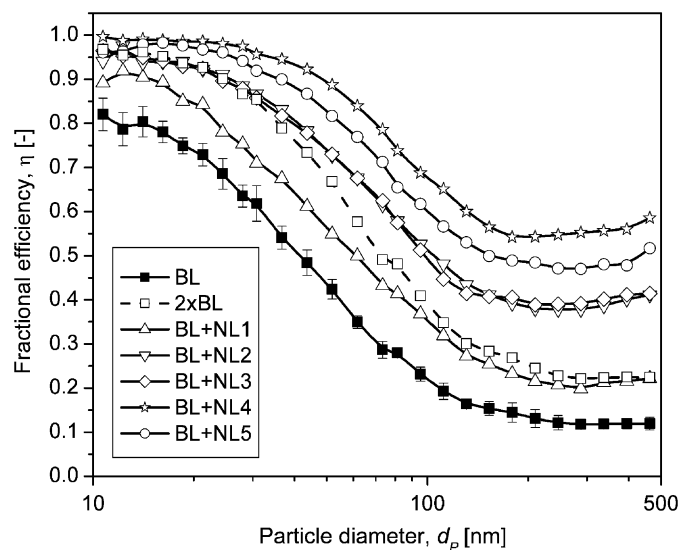


Fig. 8. The efficiencies for one and two backing layers and for the sets of the backing layer and one nanofibrous layer.

layer was tested, then the nanofibrous layer was removed and the experiment was carried out for the backing layer. The measurements of the aerosol concentration and the size distribution were repeated three times upstream of the filter, four times downstream of the filter and again three times at the aerosol inlet to assure that the particle concentration was stable during the entire experiment. The filters' efficiencies were determined on the basis of the mean values of the aerosol concentration of the particles with given diameter, calculated using data obtained in four samples upstream of the filter and three samples downstream of the filter (the first sample in each series was excluded since it could be influenced by the aerosol remained in the instrument or tubes after the previous sample). In the case of the backing layer, each point in Fig. 8 represents the mean value of the filter efficiency obtained from five such tests and the error bars are the standard deviations. The results shown in Fig. 8 indicate that using additional layer of the filter composed of nanofibers considerably increases the filter efficiency, especially in the range of the MPPS, where the efficiency achieves the lowest values. Only for one nanofibrous media (NL1) the efficiency of the set of this layer and the backing layer was lower than that observed for two layers of the backing filter for the particle diameters up to 100 nm. However, the NL1 was much thinner than the backing layer and, as all other nanofibrous layers, it was very porous.

The pressure drop across the filter is linearly dependent on its thickness. Fig. 9 depicts the pressure drop per unit filter thickness versus air face velocity, which was the highest for the backing filter, whereas the lowest values were observed for the most porous nanofibrous filters (NL4 and NL5).

On the basis of the experimental data of the filters' efficiencies and the pressure drops across the filters, the quality factor was calculated using Eq. (1). Fig. 10 shows the comparison of the QF values of the tested filters. It indicates that using the filter with the micrometer fibers is the least profitable, since

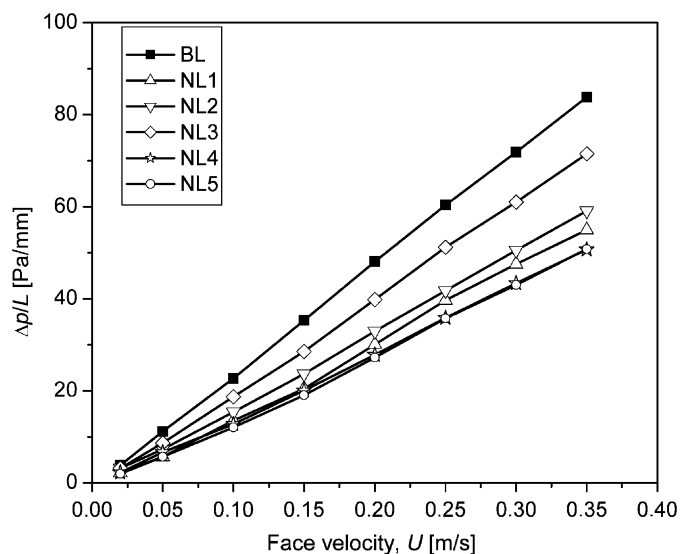


Fig. 9. Pressure drop per unit filter thickness obtained for micro- and nano-fibrous layers versus the air face velocity.

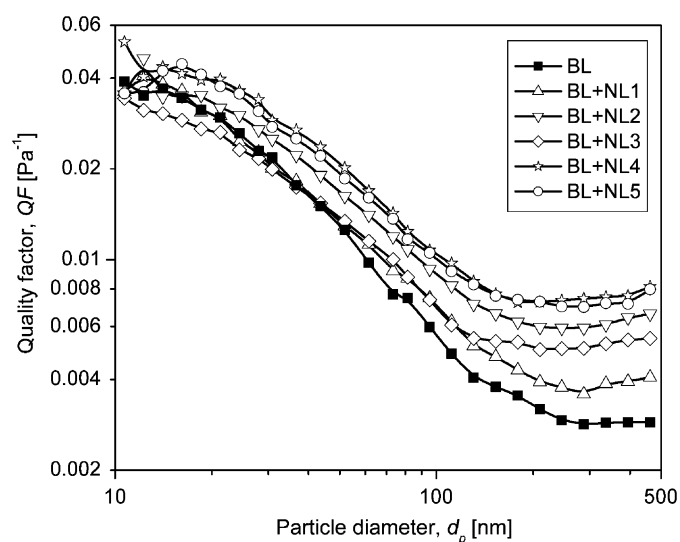


Fig. 10. The quality factor determined for the backing filter and the sets of the backing and the nanofibrous filters.

the QF values obtained for the backing filter were generally the lowest. Only using one nanofibrous layer (NL3), the quality factor for the particles smaller than about 30 nm had lower values than that for the BL. However, the pressure drop across the backing filter was relatively high comparing to others layers with nanofibers. The QF values indicate that the best solutions were the sets with nanofibrous layers NL4 and NL5, which resistances to the air flow were the lowest and their efficiencies were the highest in entire measured size-range. The count mean fiber diameters of the filters NL4 and NL5 were not the smallest among the tested nanofibrous filters; however, their equivalent fiber diameters, determined on the basis of the measured pressure drop, were the lowest. (Detailed information about the methods of evaluation of various equivalent fiber diameters may be found below).



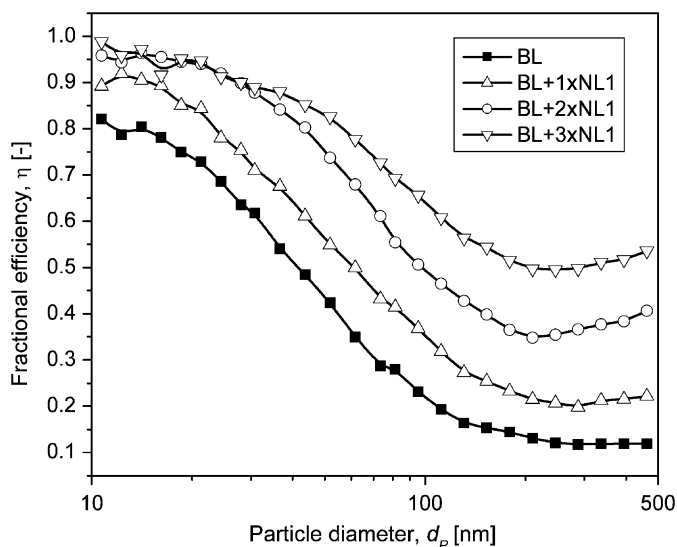


Fig. 11. Comparison of the fractional efficiency of the microfibrous filter covered with different numbers of the nanolayer NL1.

Since the filter efficiency depends on the filter thickness, the increase of the number of nanofibrous layers added to the backing layer should increase the filter efficiency. The experiments with one, two and three layers of NL1 (which is the thinnest filter among the tested ones) placed on the backing layer were carried out. The efficiencies measured for many-layer systems are presented in Fig. 11. Considerable increase of the efficiency with addition of the consecutive layers may be observed, particularly for the range of the most penetrating particles.

Comparison of the pressure drops across such sets of the filters indicates that the pressure drop for double layer of the backing filter was even a little higher than that one observed for the set of three layers—the backing layer covered with two layers of the NL1. The values of the quality factor versus particle diameter, calculated for the backing layer and the sets of the backing layer plus one and plus two nanofibrous layers, are shown in Fig. 12. These results indicate that addition of a thicker layer of the filter composed of nanofibers is profitable, therefore the bilayer filters containing the nanofibrous layers should have relatively thin backing layer and thicker layer with nanofibers. However, to avoid a fast clogging of very efficient nanofibrous layer and a rapid increase of the pressure drop, an additional layer with micrometer-sized fibers should be placed in front of the nanofibrous filter in order to capture the larger particles.

Theoretical calculations allowed anticipating an increase of the filter efficiency with decrease of the fibers diameter, which was confirmed experimentally. On the basis of experimental results, we examined how precisely the performance of the real filters composed of nanofibers may be predicted using classical theory of depth filtration.

One of the key assumptions of the classical theory of depth filtration is that the filter is homogeneous. However, the analysis of the filters' structure, presented above indicates that the tested filters were not composed of the fibers with exactly the same

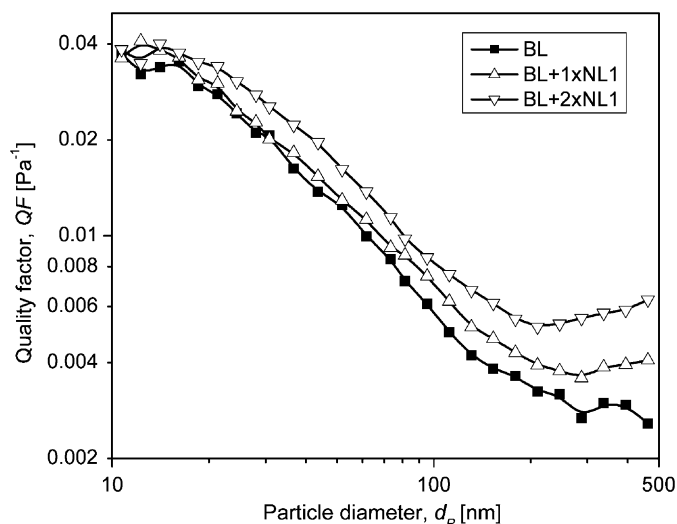


Fig. 12. The quality factor versus particle diameter, calculated for the backing layer and for the sets of the backing layer plus one and two nanofibrous layers NL1.

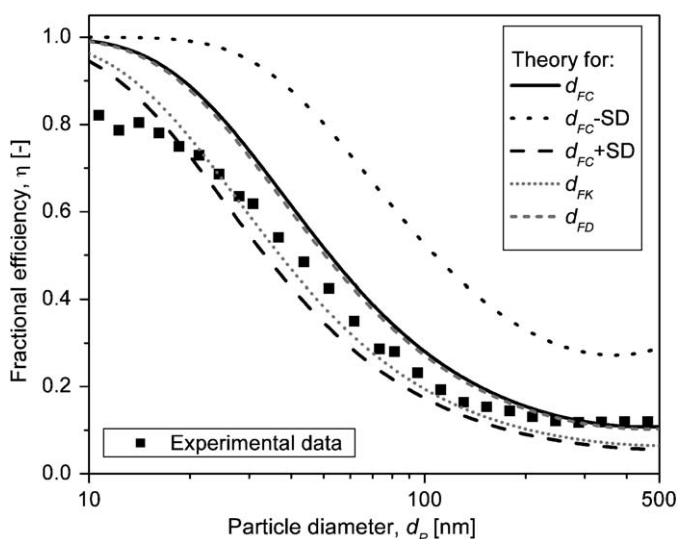


Fig. 13. Comparison of the experimental data with the results of theoretical calculations of the efficiency of the backing layer determined for the mean count fiber diameter,  $d_{FC}$ , and for the resistance-equivalent fiber diameters  $d_{FD}$  and  $d_{FK}$ . (Dashed and dotted lines show the efficiency for  $d_{FC}$  plus and minus standard deviation, respectively).

diameter. The commercial filters also usually contain the fibers of various sizes.

If the fibrous filter is composed of the fibers with various diameters it is uncertain which one should be used in the model equations. The simplest possibility is the use of the count mean (arithmetic mean) diameter,  $d_{FC}$ , to calculate the filter efficiency. Fig. 13 shows the comparison of the experimental results and theoretical predictions of the efficiency of the backing layer determined for the count mean fiber diameter (the solid line). The dashed and the dotted lines are the efficiencies of the BL calculated for  $d_{FC} \pm SD$ . The agreement

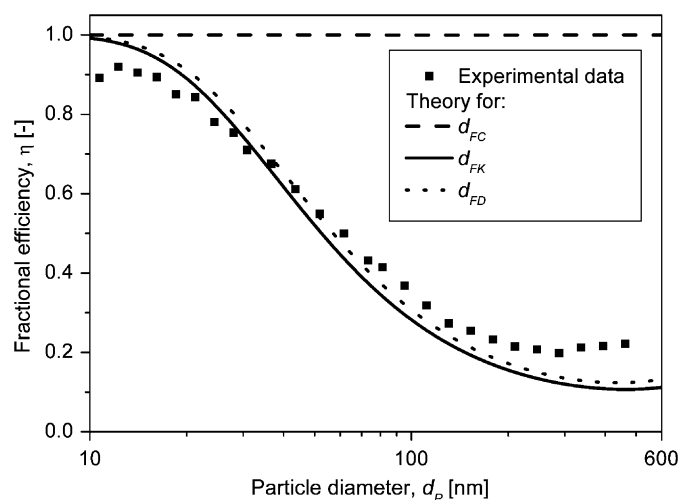


Fig. 14. Comparison of the experimental data of the efficiency for the set of filters containing BL and NL1 in series with theoretical results obtained for mean count,  $d_{FC}$ , and for the resistance-equivalent diameters  $d_{FD}$  and  $d_{FK}$ .

between experimental and theoretical data obtained for the mean count fiber diameter was not very good, although, with the exception of a few the smallest particle diameters, all experimental points are contained between the lines determined for  $d_{FC} \pm \text{SD}$ . Another fiber diameter, commonly used in calculations, is the resistance-equivalent diameter determined on the basis of the pressure drop values measured experimentally. The values of the efficiency calculated using the equivalent fiber diameters of the backing filter, obtained utilizing Davies' correlation, Eq. (8),  $d_{FD}$ , and determined from the Eq. (7) based on the Kuwabara flow model,  $d_{FK}$ , are also shown in Fig. 13. The best agreement between theoretical and experimental data was achieved in this case for the equivalent fiber diameter based on the Kuwabara cell model with slip. Thus, this diameter was used then for the calculations of the efficiency of the backing layer combined with nanofibrous layers. To calculate the resultant efficiency for a bilayer system, the count mean fiber diameters were used first in the model equations for nanofibrous layers. However, the values of the efficiency calculated on the basis of these diameters were much higher than the results of the experiments in entire measured particles size-range in the case of all tested nanofibrous filters. Further calculations were done using the resistance-equivalent diameters  $d_{FC}$  and  $d_{FK}$ . The values of the fiber diameters determined using different methods described above are listed in Table 4. For all nanofibrous filters the equivalent fiber diameters obtained on the basis of the experimental measurements of the pressure drop were much larger than the mean diameters evaluated using the SEM micrographs. The theoretical efficiencies were estimated for all kinds of the above-mentioned values of the fiber diameters. For two of the tested filters with nanofibers—NL1 (see Fig. 14) and NL3—a relatively good agreement between theoretical and experimental data was observed in some measured particles size ranges, when the resistance-equivalent fiber diameters calculated from Eqs. (7) and (8) were taken into consideration. However, the theoretical values of the efficiency of other filters were consider-

ably underestimated for such determined resistance-equivalent diameters of fibers, suggesting that the effective fiber diameter to be used in the filter efficiency calculations is smaller. These results indicate that when the filter contains the polydisperse nanofibers it is difficult to find one equivalent fiber diameter, which could be used for theoretical prediction of the filter efficiency. Moreover, the polydispersity of the filter pores, which was not investigated in this study, has also the influence on the obtained filter efficiency. The inhomogeneity of the fibrous filter was discussed by, e.g., Kirsch and Stechkina (1973), Kirsch et al. (1973, 1974), Shapiro (1996), Dhaniyala and Liu (1999, 2001a, 2001b), and Chernyakov (2004). Nevertheless, the issue of the modeling of inhomogeneous filters made of polydisperse nanofibers needs a further effort.

#### 4. Conclusions

An improved melt-blown technique for manufacturing fibrous media was developed, which allowed us to produce a wide variety of fibrous filters with controlled, well-defined structures, including conventional filters made of micrometer-sized fibers and also very porous ones composed of fibers as small as 200 nm in diameter. This technology is very competitive compared to the electrospinning method for nanofibers production since it enables one to achieve higher production rates and eliminates formation of a huge amount of toxic vapor wastes. Theoretical analysis indicates that use of nanofibrous media should be very favorable solution to filter out submicrometer-sized aerosol particles, especially these ones which penetrate the most through conventional filters composed of microfibers. Simultaneously, the theory predicts that the MPPS can be significantly reduced with the use of nanofibrous media. Experimental investigations fully confirmed these expectations. The minimum value of the quality factor determined for a combination of microfibrous backing layer and the best (from the QF criterion viewpoint) nanofibrous layer (NL4) was 2.6 times greater than the minimum value of QF for two layers of microfibrous support. Among the nanofibrous layers the fractional efficiency of the NL1 was found to be the lowest in the entire range of particle diameters. Although this filter had the lowest count mean fiber diameter, it was simultaneously the thinnest one and therefore the undesirable phenomenon of “tunneling” of the aerosol flow through zones of a higher local porosity, caused by inhomogeneous filter structure, resulted in a greater penetration of submicrometer-sized particles. For a thicker filter this effect is expected to be less important since fewer “direct passages” with large pores through the entire filter are anticipated to exist. This presumption seems to be confirmed by the fact that experimentally determined quality factor for two NL1 layers placed on the BL support was remarkably higher than that one for single NL1 filter covering the BL layer. Note also that the best nanofibrous filter (NL4) was the thickest one. Therefore, we may conclude that preferably high homogeneity of the filter structure is one of the key parameters of nanofibrous media and it can be hardly achieved in the case of too thin layers. Comparing experimental data with the predictions of the classical single-fiber theory of depth filtration we found

that this theory worked fairly well for microfibrinous support but it tremendously overestimated filtration efficiency (and pressure drop, too) for nanofibrous media. This again may be attributed to the inhomogeneity of the filter structure and to the polydispersity of fiber sizes. A better estimate of the filtration efficiency may be obtained using the resistance-equivalent fiber diameter determined from the measurements of the pressure drop. Finally, we can recommend the triple-layer design of fibrous filters dedicated to removal of polydisperse aerosol containing among others nanoparticles. The backing support layer should be rather thin, relatively densely packed and made of larger fibers with dozens of micrometers in diameter. Its role is to assure a proper mechanical strength and endurance of the entire filter. The middle layer, composed of nanofibers, may be thicker and much more porous and it is intended for precise collection of the most penetrating, submicrometer-sized particles. The front layer can be made of fibers with intermediate sizes (of the order of a few micrometers) and it should be also rather porous and thicker than the support. This layer serves not only as the mechanical shield of the delicate nanofibrous media, but it also plays an important role in collecting larger, micrometer-sized particles, protecting in such a way the middle layer against too fast clogging.

## Notation

$a_F$	filter specific area, $\text{m}^2 \text{m}^{-3}$
$A_F$	surface area of a filter sample, $\text{m}^2$
$c_{\text{down}}$	aerosol concentration downstream of a filter, # particles $\text{cm}^{-3}$
$c_{\text{up}}$	aerosol concentration upstream of a filter, # particles $\text{cm}^{-3}$
$D$	coefficient of Brownian diffusion for a particle, $\text{m}^2 \text{s}^{-1}$
$d_F$	fiber diameter, m
$d_{FC}$	mean count fiber (arithmetic mean) diameter, m
$d_{FD}$	resistance-equivalent diameter from Davies' correlation, Eq. (12), m
$d_{FK}$	resistance-equivalent diameter based on the Kuwabara model with slip, Eq. (8), m
$d_p$	aerosol particle diameter, m
$E$	total single-fiber efficiency, dimensionless
$E_D$	single fiber efficiency for diffusional mechanism, dimensionless
$E_{IR}$	single fiber efficiency for interception mechanism, dimensionless
$IR$	interception parameter, dimensionless
$Kn$	Knudsen number, dimensionless
$Kn_F$	Knudsen number for a fiber, dimensionless
$Ku$	Kuwabara number, dimensionless
$L$	filter thickness, m
$m_F$	mass of a filter sample, kg
$QF$	quality factor, $\text{Pa}^{-1}$
$P$	particle penetration through a filter, dimensionless
$Pe$	Peclet number, dimensionless
$R$	fiber radius, m

$R_0$	radius of a nozzle hole, m
$U$	face gas velocity, $\text{m s}^{-1}$

## Greek letters

$\alpha$	filter packing density, dimensionless
$\Delta p$	pressure drop, Pa
$\varepsilon$	filter porosity, dimensionless
$\eta$	filter efficiency, dimensionless
$\lambda_g$	gas mean free path, m
$\rho_F$	density of fiber's material, $\text{kg m}^{-3}$
$\rho_{SF}$	filter surface density (basis weight), $\text{g m}^{-2}$

## Acknowledgement

The work was financed from the budget means for science in 2006–2009 as a research project.

## References

- Aitken, R.J., Creely, K.S., Tran, C.L., 2004. Nanoparticles: an occupational hygiene review. Research Report 274. Edinburgh, UK, Institute of Occupational Medicine.
- Brown, R.C., 1993. Aerosol Filtration: An Integrated Approach to the Theory and Applications of Fibrous Filters. Pergamon Press, Oxford.
- Chernyakov, A.L., 2004. The influence of fluctuations on the efficiency of aerosol particle collection with fibrous filters. Colloid Journal 66 (3), 355–366.
- Davies, C.N., 1973. Air Filtration. Academic Press, London.
- Demir, M.M., Yilgor, I., Yilgor, E., Erman, B., 2002. Electrospinning of polyurethane fibers. Polymer 43, 3303–3309.
- Dhaniyala, S., Liu, B.Y.H., 1999. An asymmetrical, three-dimensional model for fibrous filters. Aerosol Science and Technology 30, 333–348.
- Dhaniyala, S., Liu, B.Y.H., 2001a. Experimental investigation of local efficiency variation in fibrous filters. Aerosol Science and Technology 34, 161–169.
- Dhaniyala, S., Liu, B.Y.H., 2001b. Theoretical modeling of filtration by nonuniform fibrous filters. Aerosol Science and Technology 34, 170–178.
- Dorman, R.G., 1966. Filtration. In: Davies, C.N. (Ed.), Aerosol Science. Academic Press, London, pp. 195–222.
- Gougeon, R., Boulaud, D., Renoux, A., 1996. Comparison of data from model fiber filters with diffusion, interception and inertial deposition models. Chemical Engineering Communications 151, 19–39.
- Gradoń, L., Podgórski, A., Bałazy, A., 2005. Filtration of nanoparticles in the nanofibrous filters. FILTECH 2005 Conference Proceedings, Wiesbaden, 11–13 October, vol. II, pp. 178–183.
- Grafe, T., Graham, K., 2002. Polymeric nanofibers and nanofiber webs: a new class of nonwovens. In: International Nonwovens Technical Conference (Joint INDA – TAPPI Conference), Atlanta, Georgia, 24–26 September.
- Grafe, T., Gogins, M., Barris, M., Schaefer, J., Canepa, R., 2001. Nanofibers in filtration applications in transportation. In: Filtration 2001 International Conference and Exposition of the INDA, Chicago, Illinois, 3–5 December.
- Graham, K., Ouyang, M., Raether, T., Grafe, T., McDonald, B., Knauf, P., 2002. Polymeric nanofibers in air filtration applications. Fifteenth Annual Technical Conference & Expo of the American Filtration & Separations Society, Galveston, Texas, 9–12 April.
- Hinds, W.C., 1999. Aerosol Technology. Wiley, New York.
- Huang, Z.M., Zhang, Y.Z., Kotaki, M., Ramakrishna, S., 2003. A review on polymer nanofibers by electrospinning and their applications in nanocomposites. Composites Science and Technology 63, 2223–2253.
- International Organisation for Standardisation (ISO), 2004. Occupational ultrafine aerosol exposure characterisation and assessment. Draft technical report number 6. Particle size selective sampling and analysis (workplace air quality). ISO/TC146/SC2WG1.

- Jaroszcyk, T., Liu, Z.G., Schwartz, S.W., Holm, C.E., Badeau, K.M., Janikowski, E., 2005. Direct flow air filters—a new approach to high performance engine filtration. In: FILTECH 2005 Conference Proceedings, Wiesbaden, 11–13 October, vol. II, pp. 234–244.
- Kalayci, V.E., Patra, P.K., Kim, Y.K., Ugbohue, S.C., Warner, S.B., 2005. Charge consequences in electrospun polyacrylonitrile (PAN) nanofibers. *Polymer* 46, 7191–7200.
- Kirsch, A.A., Stechkina, I.B., 1973. Pressure drop and diffusional deposition of aerosol in polydisperse model filter. *Journal of Colloid and Interface Science* 43 (1), 10–16.
- Kirsch, A.A., Stechkina, I.B., Fuchs, N.A., 1973. Effect of gas slip on the pressure drop in fibrous filters. *Journal of Aerosol Science* 4, 287–293.
- Kirsch, A.A., Stechkina, I.B., Fuchs, N.A., 1974. Gas flow in aerosol filters made of polydisperse ultrafine fibres. *Journal of Aerosol Science* 5, 39–45.
- Kosmider, K., Scott, J., 2002. Polymeric nanofibres exhibit an enhanced air filtration performance. *Filtration & Separation* July/August, 20–22.
- Park, H.S., Park, Y.O., 2005. Filtration properties of electrospun ultrafine fiber webs. *Korean Journal of Chemical Engineering* 22 (1), 165–172.
- Podgórski, A., 2002. On the Transport, Deposition and Filtration of Aerosol Particles: Selected Problems. Publishing House of the Warsaw University of Technology, Warsaw.
- Shapiro, M., 1996. An analytical model for aerosol filtration by nonuniform filter media. *Journal of Aerosol Science* 27 (2), 263–280.
- Ward, G., 2005. Nanofibres: media at the nanoscale. *Filtration & Separation*, September, 22–24.